Review

MRI and PET Alterations in Adult Skull-Base Tumors: A Narrative Review of Proton versus Photon Radiotherapy

Gokoulakrichenane Loganadane * , Valentin Calugaru , Dimitri Anzellini , Benjamin Nicaise , Sarah Mezghani , Nam P Nguyen , Brandi R Page

Posted Date: 9 January 2026

doi: 10.20944/preprints202601.0677.v1

Keywords: skull-base tumor; radiation indued brain injury (RIBI); radiation-induced contrast enhancement (RICE); proton therapy; relative biological effectiveness; radiation necrosis

 doi:10.20944/preprints202601.0677.v1

Review

MRI and PET Alterations in Adult Skull-Base Tumors: A Narrative Review of Proton versus Photon Radiotherapy

Gokoulakrichenane Loganadane [1,*], Valentin Calugaru [1], Dimitri Anzellini [2], Benjamin Nicaise [1], Sarah Mezghani [3], Nam P Nguyen [4] and Brandi R Page [5]

[1] Department of Radiation Oncology, Institut Curie, 75005 Paris; France
[2] Department of Radiation Oncology, Sant'Andrea Hospital, Sapienza University, 00189 Rome, Italy
[3] Department of Imaging, Institut Curie, 75005 Paris, France
[4] Department of Radiation Oncology, Howard University, Washington, DC 20060, USA
[5] Department of Radiation Oncology, Johns Hopkins University School of Medicine, Baltimore, Maryland, USA
* Correspondence: gloganadane@gmail.com

Abstract

Background: Radiotherapy is an essential component for the treatment of skull skull-base tumours. However, radiation-induced brain injury (RIBI) appearing on magnetic resonance imaging (MRI) as pseudoprogression, radiation-induced contrast enhancement (RICE), radiation necrosis, and other contrast-enhancing brain lesions—remains an important late toxicity which is not very well characterized. Clarifying adult-specific patterns, the role of positron emission tomography (PET), and differences between proton and photon therapy is clinically relevant. **Methods:** Narrative review of peer-reviewed literature to 1 October 2025 focused on adult chordoma, chondrosarcoma, meningioma, adenoid cystic carcinoma, pituitary adenoma, craniopharyngioma, undifferentiated carcinoma of nasopharyngeal type (UCNT), and germinoma. **Results:** Radiation-induced brain injury (RIBI) may range from early transient brain oedema/enhancement to late necrosis. Lesions cluster in temporal and frontal lobes after skull-base irradiation. Proton therapy generally reduces high-dose exposure versus photons and is associated with fewer severe necrotic events, though asymptomatic RICE is common. Advanced MRI (diffusion, perfusion, spectroscopy, ASL, amide proton transfer) and positron emission tomography (PET) with Fluorodeoxyglucose (FDG) and amino-acid tracers aid distinction between treatment effect and progression. Risk reflects dose–volume metrics, prior irradiation, and patient comorbidities. **Conclusions:** MRI/PET alterations after skull-base radiotherapy vary by modality, dose, and tumor context. Integrating multimodal imaging with clinical factors should guide surveillance and management; prospective validation is needed.

Keywords: skull-base tumor; radiation indued brain injury (RIBI); radiation-induced contrast enhancement (RICE); proton therapy; relative biological effectiveness; radiation necrosis

1. Introduction

Epidemiology and treatment of skull-base tumours

The skull base represents one of the most intricate anatomical regions in the human body, serving as the structural floor of the cranial cavity and the roof of the aerodigestive tract [1]. It encompasses the clivus, jugular foramen, temporal bone, petrous apex, and the sellar and parasellar regions. This confined space is traversed by critical neurovascular structures, including the cranial nerves, the internal carotid arteries, the brainstem, and the optic apparatus [2]. Consequently, tumours arising in this region present a significant challenge for local control and functional preservation due to their close proximity to critical neural structures.

 doi:10.20944/preprints202601.0677.v1

The spectrum of skull-base pathology is broad. Primary bone malignancies such as chordomas and chondrosarcomas are locally aggressive, arising from notochordal remnants and cartilaginous precursors, respectively. Benign or borderline neoplasms, including meningiomas, pituitary adenomas, and craniopharyngiomas, often compress vital structures, necessitating intervention despite their non-malignant histology [3,4]. Furthermore, malignant epithelial tumours like adenoid cystic carcinoma (ACC) of the minor salivary glands and undifferentiated carcinoma of nasopharyngeal type (UCNT) frequently invade the skull base via perineural spread, tracking along cranial nerves into the cavernous sinus and Meckel's cave. Although individual skull-base tumour types are rare, their cumulative burden on the healthcare system and patient quality of life is significant. The proximity of these tumours to eloquent neural structures necessitates high-precision therapies that can deliver tumouricidal doses while respecting the tolerance of the adjacent brain parenchyma. Although individual skull-base tumour types are rare, their cumulative burden on the healthcare system and patient quality of life is significant. The proximity of these tumours to eloquent neural structures necessitates high-precision therapies that can deliver tumouricidal doses while respecting the tolerance of the adjacent brain parenchyma.

Radiotherapy (RT) is critical in the management of skull-base tumours,. It is used as sole therapy for unresectable disease or as an adjuvant treatment following subtotal resection. The technological evolution of RT has been driven by the imperative to maximize the therapeutic ratio [5].

Modern photon techniques, such as intensity-modulated radiotherapy (IMRT) and volumetric-modulated arc therapy (VMAT), utilize computer-optimized multi-leaf collimators to shape the radiation dose to the target volume [6]. While these techniques achieve high conformality, photons inevitably exit the patient, depositing an "exit dose" along their path. In skull-base irradiation, this results in a "bath" of low-to-intermediate dose radiation delivered to the temporal lobes, frontal lobes, and brainstem, potentially contributing to late cognitive toxicity and secondary malignancies.

Proton-based therapy (PBT) has emerged as a superior alternative for many skull-base indications. Protons exploit the Bragg peak phenomenon, where charged particles deposit the majority of their energy at a specific depth before coming to a rapid halt [7,8]. This unique physical property allows for the elimination of exit dose, significantly reducing the integral dose to the brain and sparing organs at risk for complications (OARs) such as the cochlea, hippocampus, and temporal lobes. For radioresistant tumours like chordomas, which often require doses in the range of 60–74 Gy RBE (Relative Biological Effectiveness), Thus, PBT enables radiatiodose escalation that would be unsafe with photons [9].

Proton therapy exploits the Bragg peak to reduce exit dose, offering better sparing of normal tissues. Carbon-ion therapy offers high relative biological effectiveness (RBE) but may increase necrosis risk. While modern techniques improve tumour control, radiation-induced brain injury remains a serious complication. Skull base osteoradionecrosis specifically is a rare but potentially devastating complication of radiotherapy for head and neck malignancies, characterized by hypovascularity, hypoxia, and necrosis [10]. The severity of this condition stems from the skull base's proximity to vital neurovascular structures, where progressive bone destruction can lead to catastrophic sequelae such as cranial nerve palsies, meningitis, or fatal carotid artery hemorrhage. Adult patients often require high doses (60–74 Gy_RBE) for chordomas, and re-irradiation is common in recurrent meningiomas or pituitary adenomas, further increasing the complication risk. Understanding MRI alterations and their clinical significance in the adult population is crucial for early detection and management.

Anatomically, skull-base tumours are surrounded by eloquent neural structures. Tumours of the clivus about the medial temporal lobes and brainstem, whereas jugular foramen tumours lie near the cerebellum and lower cranial nerves. Lesions such as adenoid cystic carcinoma may track along cranial nerves into the cavernous sinus and Meckel's cave. Achieving tumouricidal dose while sparing the temporal lobes and optic pathways requires meticulous planning. Proton therapy and advanced IMRT allow steep dose gradients, but uncertainties in proton range and daily anatomical changes can lead to unexpected dose to critical tissues [11,12]. For example, anatomic alterations

 doi:10.20944/preprints202601.0677.v1

during treatment, such as the resolution of post-operative edema or daily variation of the sinus mucous may reduce the density of tissue the beam traverses. Without adaptation, this allows the beam's high-dose Bragg peak to penetrate deeper than planned, potentially overdosing the adjacent neurological structures.

Thus, clinicians must be familiar with expected imaging changes and maintain vigilance during treatment planning and follow-up. Awareness of tumour-specific anatomy also informs risk assessment; for example, radiation therapy for pituitary adenoma rarely leads to temporal lobe injury but may can cause optic nerve enhancement mimicking tumour recurrence, and potential mismanagement.

Proton range uncertainties and daily anatomical changes can significantly alter dose delivery to critical structures like the brainstem, particularly when using anterior beams for skull base tumors. Specific examples that could drastically affect end ranging and dose to critical structures could include weight loss, sinus filling, and tissue density variations which can all directly impact proton beam attenuation and range. When patient separation decreases due to weight loss, the water equivalent path length (WEPL) to the target shortens, potentially causing the Bragg peak to overshoot the intended target and deposit high doses in structures beyond it, such as the brainstem when using anterior beams [13]. This is particularly problematic because the distal edge of the Bragg peak, which may abut critical neurological structures, has been measured to have RBE values as high as 6.0 in vitro, though in clinical practice an RBE of 1.1 is commonly calculated and has not shown toxicities expected at that magnitude [14]. Another example that may affect skull base proton therapy includes sinusitis or inconsistent filling of mucous of sinuses if there is an anteriorly located beam. This is problematic because when the nasal cavity or sinuses fill with mucus during upper respiratory infections or sinusitis, the tissue density along the beam path increases. This increased density causes the proton beam to lose energy more rapidly, resulting in a shortened range the Bragg peak, potentially underdosing the intended target. Conversely, when air cavities are present (normal state), the beam travels further [15]. This is one of the reasons anterior proton fields are generally avoided.

Increased body mass index with thicker necks and variable neck skin folding can create unintended bolus effects that alter the beam's entrance characteristics and range. Tissue folds or increased subcutaneous tissue effectively increase the WEPL to deeper structures, potentially causing the beam to stop short of the target or shifting high-dose regions posteriorly toward the brainstem. This is compounded by the fact that proton therapy can result in significant entrance dose with loss of skin-sparing effects, especially for targets requiring significant beam modulation. Complex treatment planning, quality assurance CT established at an acceptable frequency every 1-2 weeks, highly trained physics and therapy staff, with replanning capability multiple times during treatment is a must in any of these cases. Treatment planning should involve choosing shortest beam paths possible, avoiding surgical or dental hardware, and minimizing traversing of hollow organs [14].

This review aims to summarise MRI alterations in adult patients with skull-base tumours treated with proton and photon radiotherapy, delineate pathophysiological mechanisms and clinical risk factors, compare outcomes between modalities, and highlight advanced MRI and PET techniques for differentiating radiation injury from tumour recurrence. Emphasis is placed on chordomas, meningiomas, chondrosarcomas, adenoid cystic carcinoma, pituitary adenoma, craniopharyngioma, UCNT and germinoma, but data from other skull-base tumours are included when relevant. Only adult patients (>18 years) are considered, as paediatric responses differ significantly.

2. Materials and Methods

A literature search was performed up to 1 October 2025 using PubMed, Scopus and Web of Science. Search terms included combinations of "skull base tumour", "radiation-induced brain injury", "radiation necrosis", "pseudoprogression", "contrast-enhancing brain lesion", "proton therapy", "photon therapy", "MRI", "PET", and each tumour type. Reference lists of selected articles were hand-searched. Eligible studies reported on adult patients treated with radiotherapy for skull-

 doi:10.20944/preprints202601.0677.v1

base tumours and included imaging data on radiation-induced brain injury. Both prospective and retrospective series, case reports and review articles were considered. Emphasis was placed on peer-reviewed sources with accessible full texts from the connected environment. When direct access to an article was not possible due to dynamic content or paywalls, data were synthesised from accessible reviews or abstracts. Citations from previous windows of the connected environment were used; direct quoting of search results was avoided.

3. Results

3.1. Pathophysiology of Radiation-Induced Brain Injury

Radiation injury results from complex interactions between endothelial damage, glial cell injury, inflammation, and impaired repair mechanisms. The initial insult involves free radical generation and DNA damage leading to vascular endothelial apoptosis. Cerebral vessels develop hyalinisation, capillary loss, and blood–brain barrier breakdown [16]. Cytokines such as vascular endothelial growth factor (VEGF), tumour necrosis factor-α and interleukins are released, promoting oedema, neovascularisation and demyelination. In chronic phases, progressive vascular occlusion and hypoxia cause coagulative necrosis [16]. The severity depends on total dose, dose per fraction, irradiated volume, and tissue sensitivity.

3.2. Categories of Injury

Radiation-induced brain injury can be categorised by timing and imaging features

3.2.1. Acute Injury (Within Hours to Days)

Rare in high-precision skull-base radiotherapy because the brain receives fractionated doses. When present, it reflects blood–brain barrier disruption with vasogenic oedema and T2/FLAIR hyperintensity. It usually resolves spontaneously and seldom causes lasting deficits [17].

3.2.2. Early Delayed Injury (1–6 Months)

Characterized by demyelination and transient oligodendrocyte damage. MRI shows diffuse T2/FLAIR hyperintensity in white matter with minimal or patchy contrast enhancement; involvement of deep temporal lobes is typical after skull-base irradiation. Pseudoprogression, defined as transient new or enlarged enhancing lesions within months of therapy, belongs to this category. It occurs in 20–30% of patients, particularly when concurrent chemotherapy (e.g., temozolomide) is used [18]. Pseudoprogression tends to peak around three months and resolves over subsequent months.

3.2.3. Late Delayed Injury (>6 Months)

Includes RICE and radiation necrosis. RICE encompasses new contrast-enhancing lesions that may or may not have clinical symptoms; lesions often appear as small nodular enhancements or rim-like patterns in the temporal or frontal lobes and may improve or resolve spontaneously [19]. Radiation necrosis represents irreversible parenchymal destruction with cavitation and “soap-bubble” or ring enhancement [20]. Necrosis often occurs 12–36 months after therapy, though cases have been reported up to 10 years. The LENT-SOMA (Late Effects in Normal Tissues—Subjective, Objective, Management and Analytic) classification grades injury from Grade 1 (radiological changes without symptoms) to Grade 4 (severe necrosis requiring surgical intervention)[[21].

3.3. MRI Alterations in Skull-Base Tumours

3.3.1. Pseudoprogression and RICE

Pseudoprogression and RICE are forms of early or intermediate radiation injury that mimic tumour progression [22]. They present as new or enlarging contrast-enhancing lesions with T2/FLAIR hyperintensity and mass effect. In prospective proton therapy cohorts, RICE incidence is 15%, with

 doi:10.20944/preprints202601.0677.v1

onset at median 11.8 months and resolution over nine months [19]. High dose to small volumes (D1% ≥ 57.6 Gy_RBE), prior radiation and diabetes mellitus increase risk [19]. In addition to diabetes mellitus, classical vascular risk factors including older age, hypertension, and smoking independently increase the risk of RICE in patients undergoing proton therapy to the skull base [23].

Another proton cohort reported asymptomatic RAIC (radiation-associated image changes) in 17.3% of patients; 45.5% of lesions resolved or improved, and the 3-year actuarial rate was 14.3%[24]. Lesions occurred predominantly in the temporal (14/127), frontal (6/127) and cerebellar (2/127) lobes and were small (median 0.5 cc)[24].

3.3.2. Radiation Necrosis

Radiation necrosis is the most severe late effect, representing irreversible tissue destruction. MRI typically shows ring-enhancing lesions with central necrosis and surrounding oedema. Differentiating necrosis from tumour recurrence is challenging because both exhibit contrast enhancement. Particle therapy series suggest lower necrosis rates than photon therapy. In a study of skull-base chordoma and chondrosarcoma treated with proton or carbon therapy, 21.5% experienced temporal-lobe reactions and 13.9% developed necrosis [25]. Median onset was 20 months, and lesions occurred at median doses of 63.8 Gy_RBE [25]. Univariate analysis showed that larger irradiated volumes (V_60–70), higher D_max and older age increased necrosis risk [25].

Photon therapy for nasopharyngeal carcinoma and other head-and-neck cancers has long been associated with temporal-lobe necrosis. Classic series using two-dimensional techniques reported necrosis rates of 2–10%. IMRT reduces but does not eliminate risk; rates range from 2–5%. Proton therapy further lowers high-dose volumes. In a mixed head-and-neck cohort receiving at least 40 Gy_RBE to the brain, RAIC occurred in 17.3%, mostly asymptomatic, with 3-year incidence 14.3%; high brain doses (V_70Gy>0.17 cc) strongly predicted RAIC [25]. In a prospective PBT study, symptomatic RICE accounted for 4.5%, and previous in-field irradiation predicted symptoms [19]. Another PBT series found temporal-lobe injury in 10.4% of patients receiving 63–74 Gy_RBE, with correlation between high-dose volume and injury but no definite dose threshold [26].

Clinical manifestations of necrosis depend on lesion location. Temporal-lobe injury may cause memory impairment, psychomotor slowing, or seizures; such as temporal-lobe epilepsy [27]. Cranial nerve deficits and brainstem symptoms occur with lesions near the cavernous sinus or pontine region. Management includes corticosteroids, anti-epileptics, bevacizumab, hyperbaric oxygen, and, in severe cases, surgical resection. The 2019 particle-therapy review emphasised that protons have lower necrosis incidence (17% for protons vs 64% for carbon ions) and shorter latency than carbon ions [28].

3.3.3. Contrast-Enhancing Brain Lesions (CEBL) and RIBI Spectrum

The term CEBL is increasingly used to capture heterogeneous lesions with contrast enhancement on MRI after radiotherapy. These include pseudoprogression, RICE, necrosis and small vascular malformations. As imaging and survivorship improve, recognition of subtle CEBL becomes more common. Lesions may appear years after therapy and can wax and wane. The LENT-SOMA system provides guidance on severity, but standardised nomenclature across institutions is lacking. For research, RIBI can be graded by size, symptoms and necessity of intervention.

3.4. Tumour-Specific Considerations

3.4.1. Chordoma and Chondrosarcoma

Chordomas and chondrosarcomas arise from remnants of the notochord or cartilaginous skull base. They are locally aggressive and require high-dose radiation. Proton therapy is often combined with surgical resection. In a prospective analysis of chordoma/chondrosarcoma patients (n = 144) receiving protons or carbon ions, 21.5% developed temporal-lobe reactions and 13.9% had necrosis [29]. Chondrosarcoma patients had slightly lower rates (18% reactions, 12% necrosis) with median

 doi:10.20944/preprints202601.0677.v1

latency 14 months [29]. Univariate analysis identified D_max, D_mean, volumes receiving ≥70 Gy_RBE and patient age as significant risk factors. Another review noted that the probability of temporal-lobe necrosis in chordoma patients is ~8% at two years and 13% at five years; MRI shows T2 hyperintensity in the anterior temporal lobe with cortical atrophy [30].

3.4.2. Meningioma

High-grade or recurrent meningiomas often require adjuvant radiotherapy or re-irradiation [31]. Proton therapy can deliver escalated doses while sparing normal tissues. Data on radiation-induced brain injury in meningioma is limited; however, high-dose volumes and prior irradiation increase risk. Because meningiomas are often adjacent to the temporal lobe or cavernous sinus, caution is needed when planning.

3.4.3. Adenoid Cystic Carcinoma and UCNT

Adenoid cystic carcinoma of the skull base originates from minor salivary glands and often exhibits perineural spread. Photon radiotherapy with IMRT or proton therapy is commonly used. Pseudoprogression and RICE may be mistaken for perineural tumour spread. UCNT/nasopharyngeal carcinoma has historically been treated with photons, leading to high rates of temporal-lobe necrosis, particularly in endemic regions. The introduction of IMRT and, more recently, proton therapy has significantly decreased necrosis risk. Reports indicate that RAIC after proton therapy is largely asymptomatic and resolves over time [25]. However, long-term comparative data for adenoid cystic carcinoma and UCNT are scarce.

3.4.4. Pituitary Adenoma and Craniopharyngioma

Pituitary adenomas and craniopharyngiomas lie close to the optic apparatus and hypothalamus. Stereotactic photon radiotherapy or proton therapy is used when surgery is incomplete. Radiation-induced injury may affect adjacent temporal lobes, optic tracts or hypothalamus. Pseudoprogression may occur in the optic chiasm or hypothalamic region and must be distinguished from tumour enlargement [19]. Because these tumours typically receive lower doses than chordomas (~45–54 Gy), significant necrosis is rare; however, re-irradiation increases risk.

3.4.5. Germinoma and Other Germ Cell Tumours

Intracranial germinomas often involve the suprasellar or pineal region. While proton therapy is increasingly used, adult germinoma data on radiation injury remain limited because of high cure rates and relatively low doses (36–45 Gy). Pseudoprogression can occur after chemoradiation but usually resolves.

3.5. Comparative Evaluation of Proton versus Photon Therapy

3.5.1. Dosimetric Advantages and Clinical Outcomes

Proton therapy spares normal tissue by depositing most of its energy at the Bragg peak, resulting in lower integral dose to the brain. Comparative planning studies consistently show that protons reduce high-dose volumes to temporal and frontal lobes compared with photons for skull-base tumours. Clinically, this translates into lower rates of RIBI. In the prospective PBT study, RICE incidence was 15%, and symptomatic RICE 4.5%; dose to 1% of the CNS (>57.6 Gy_RBE) significantly increased risk [19]. For head-and-neck cancers, RAIC occurred in 17.3% of proton patients but lesions were small and often resolved [32]. Conversely, carbon-ion therapy has higher RBE and may cause more necrosis; a review reported necrosis rates of 17% for protons versus 64% for carbon ions [33].

Photon therapy remains widely used. IMRT reduces temporal-lobe doses compared with older techniques but still exposes larger volumes to intermediate doses. Nasopharyngeal carcinoma series using photons report temporal-lobe necrosis rates of 2–5%, with risk increasing for total dose >70 Gy and concurrent chemotherapy. Re-irradiation or brachytherapy further elevate risk. In chordoma

 doi:10.20944/preprints202601.0677.v1

patients, photon therapy may require large margins because of proximity to brainstem, leading to more frequent necrosis. Consequently, proton therapy is considered standard for many skull-base tumours.

3.5.2. Dose–Volume Risk Factors

Across modalities, the risk of MRI alterations correlates with high-dose volumes. Significant metrics include Dmax (maximum point dose), V60–70Gy (volume receiving ≥60–70 Gy_RBE), Dmean and dose to 1% of the CNS. In the chordoma/chondrosarcoma study, higher Dmax and V70 values predicted temporal-lobe reactions and necrosis [29]. Similarly, the prospective PBT study found that D1% > 57.6 GyRBE increased RICE risk [19]. Age and diabetes were additional risk factors. A head-and-neck proton study demonstrated that V_70 ≥ 0.17 cc was associated with a 63% RAIC rate [25]. These findings support strict dose constraints to the temporal and frontal lobes.

3.5.3. Clinical Risk Factors

Clinical factors contribute to susceptibility. Older age correlates with reduced vascular repair and increased necrosis [34]. Diabetes and hypertension contribute to microvascular injury and may heighten risk [28]. Previous cranial irradiation predisposes to necrosis; in the PBT study, prior in-field radiation significantly increased symptomatic RICE [19].Tumour location influences injury pattern; clival tumours risk temporal-lobe injury, whereas jugular foramen tumours may affect the cerebellum.

3.6. Advanced Imaging Techniques

Standard MRI sequences (T1-weighted, T2/FLAIR and gadolinium-enhanced T1) provide excellent anatomical detail but may not reliably distinguish radiation injury from tumour recurrence. Advanced MRI techniques offer quantitative biomarkers.

3.6.1. Diffusion-Weighted Imaging (DWI)

DWI measures Brownian motion of water molecules. Radiation necrosis typically shows increased apparent diffusion coefficient (ADC) due to necrotic tissue and oedema, whereas recurrent tumour often exhibits lower ADC because of hypercellularity. However, overlap exists, particularly in pseudoprogression where ADC values may be intermediate. Diffusion tensor imaging (DTI) can detect white-matter tract disruption in temporal-lobe injury and may assist in planning re-irradiation [35–37].

3.6.2. Perfusion-Weighted Imaging (PWI)

Dynamic susceptibility contrast (DSC) and dynamic contrast-enhanced (DCE) PWI measure relative cerebral blood volume (rCBV) and permeability. Recurrent tumour shows increased rCBV due to neovascularisation; necrosis and RICE demonstrate low rCBV. A threshold rCBV ratio <0.7 differentiates necrosis from recurrence with high sensitivity in glioma literature, though skull-base data are sparse. Arterial spin labelling (ASL) provides non-contrast perfusion and may help in patients with renal impairment [38].

3.6.3. Magnetic Resonance Spectroscopy (MRS)

MRS assesses metabolic profiles. Recurrent tumour typically exhibits high choline peaks and reduced N-acetylaspartate (NAA), whereas necrosis shows lipid and lactate peaks with low choline. In skull-base tumours, MRS can be challenging due to bone–air interfaces but remains valuable when feasible [39].

Amide proton transfer (APT) and chemical exchange saturation transfer (CEST) imaging. APT quantifies endogenous amide protons related to mobile proteins and peptides. Preliminary studies suggest that APT signal intensity is higher in tumour recurrence than in radiation necrosis. CEST

 doi:10.20944/preprints202601.0677.v1

imaging may also detect pH changes in necrotic tissue. These techniques are investigational but hold promise for early detection [40].

3.6.4. Radiomics and Artificial Intelligence

Radiomics extracts quantitative features (texture, shape, intensity) from MRI. Machine-learning models integrating radiomic features and clinical data have shown good performance in differentiating necrosis from recurrence. Although data are limited for skull-base tumours, radiomics could improve risk stratification and guide follow-up intervals [36].

3.6.5. PET Imaging

PET provides metabolic information complementary to MRI. 18F-FDG PET measures glucose metabolism; recurrent tumour generally demonstrates high uptake, whereas necrosis shows low uptake due to tissue death. However, high baseline brain glucose uptake in the temporal lobe reduces specificity. Amino-acid PET tracers such as 18F-fluoroethyl-L-tyrosine (18F-FET), 11C-methionine (11C-MET) and 18F-fluoro-L-dihydroxyphenylalanine (18F-FDOPA) offer better lesion-to-background contrast because normal brain has low amino-acid uptake. Studies in gliomas indicate that FET-PET differentiates recurrence from radiation necrosis with sensitivity >80% [41]. In skull-base tumours, FET- or MET-PET helps evaluate lesions adjacent to the cortex or skull base and may identify early pseudoprogression. 18F-FMISO PET assesses hypoxia and may predict necrosis risk by identifying hypoxic areas susceptible to radiation injury. Combining PET and MRI (PET/MRI) allows simultaneous structural and metabolic assessment and has potential to guide adaptive radiotherapy [42]. More prospective studies are needed.

18F-FET has a half-life of 110 min and is widely available compared with 11C tracers that require on-site cyclotron. High lesion-to-background ratios (often >2) allow detection of small lesions. 18F-FDOPA, originally developed for movement disorders, accumulates in catecholamine-producing tissues and has shown utility for head-and-neck tumours. In adenoid cystic carcinoma and nasopharyngeal carcinoma, FDOPA-PET may reveal perineural spread beyond the field of MRI. 18F-FMISO and other nitroimidazole tracers accumulate in hypoxic cells; hypoxia predisposes to radioresistance and may predict areas at risk for necrosis when irradiated [36].Preliminary studies suggest that high FMISO uptake before radiotherapy correlates with subsequent necrosis, although data for skull-base tumours are limited. Hybrid PET/MRI scanners offer co-registration and reduced examination time, enabling longitudinal monitoring of metabolic changes alongside structural MRI. As PET tracers evolve (e.g., 18F-fluciclovine), their role in skull-base tumour imaging will likely expand.

3.6.6. Evolution of Lesions over Time

Radiation-induced lesions evolve dynamically. Pseudoprogression typically peaks within three months of therapy and resolves by six months [43]. RICE lesions may appear as small nodules or patchy enhancement at 6–18 months and often resolve by 12–24 months [36]. Radiation necrosis usually manifests 1–3 years post-therapy but can develop as late as 10 years; lesions may expand and then stabilise or regress. In proton cohorts, many RICE lesions improved or resolved spontaneously, highlighting the importance of watchful waiting [25]. However, symptomatic necrosis may progress, requiring intervention.

3.7. Clinical Management

Management depends on severity and symptoms. Observation is appropriate for small, asymptomatic RICE lesions because many regress. Corticosteroids reduce oedema but have systemic side-effects; they are used short-term for symptomatic pseudoprogression or RICE. Anti-angiogenic therapy with bevacizumab has been shown to reduce symptoms and radiological lesions by decreasing VEGF-mediated permeability. Hyperbaric oxygen and pentoxifylline with vitamin E

 doi:10.20944/preprints202601.0677.v1

have anecdotal benefits. Boswellia serrata extract, particularly its active component acetyl-11-keto-β-boswellic acid (AKBA), shows preliminary evidence for reducing cerebral edema associated with brain radiotherapy, but there is insufficient evidence to support its use specifically for treating established radiation necrosis. Relevant clinical evidence comes from a small prospective, randomized, double-blind, placebo-controlled trial of 44 patients with primary or secondary malignant cerebral tumors receiving radiotherapy. Patients received either Boswellia serrata 4200 mg/day or placebo during radiation treatment. A reduction in brain edema of >75% was found in 60% of patients receiving BS compared to 26% receiving placebo (p=0.023), measured by T2-weighted MRI immediately after radiotherapy completion [44].

Surgical resection is reserved for life-threatening mass effect or when diagnosis is uncertain. The potential of proton therapy to decrease necrosis supports its use for re-irradiation when feasible.

3.8. Future Directions

Despite advances, several gaps remain. Standardised terminology for radiation-induced lesions (e.g., pseudoprogression, RICE, RAIC, CEBL) is needed to facilitate comparisons. Prospective registries capturing detailed dose–volume metrics, imaging findings, and clinical outcomes across tumour types and modalities will clarify risk factors. Integration of advanced MRI, PET and radiomics into surveillance protocols could enable earlier detection and personalised follow-up intervals. New systemic therapies (e.g., immune checkpoint inhibitors) may interact with radiation, altering pseudoprogression incidence; understanding these interactions in skull-base tumours warrants investigation. Finally, exploring the role of carbon-ion therapy with improved dose painting techniques may reduce necrosis while maintaining high control rates [45].

Table 1. Categories of radiation-induced brain injury and their MRI characteristics.

Category	Typical onset	MRI features	Example incidence and notes
Acute injury	Hours to days	Diffuse T2/FLAIR hyperintensity representing vasogenic oedema	Rare with fractionated skull-base radiotherapy
Early delayed injury	1–6 months	Diffuse T2/FLAIR hyperintensity with minimal or patchy enhancement; reflects demyelination and oligodendrocyte damage	Often resolves spontaneously; may transition to pseudoprogression
Pseudoprogression	Weeks to months (peak ≈3 months)	New or enlarging contrast-enhancing lesions with T2/FLAIR hyperintensity and mass effect	Occurs in ~20–30% of patients, particularly with concurrent chemotherapy
RICE / RAIC	6–18 months (median onset ≈11.8 months)	Small nodular or patchy contrast-enhancing lesions (usually <1 cc), most commonly in temporal or frontal lobes	RICE incidence ≈15% in prospective proton cohorts; RAIC reported in 17.3% of head-and-neck patients with a 3-year actuarial rate of 14.3%.

 doi:10.20944/preprints202601.0677.v1

			Many lesions resolve over ~9 months
Radiation necrosis	>6 months (typically 12–36 months; reported up to 10 years)	Ring-enhancing lesions with central necrosis ("soap-bubble" appearance) and surrounding oedema	In chordoma/chondrosarcoma cohorts, 13.9% developed necrosis; photon IMRT series report ~2–5%, older techniques 2–10%; incidence substantially higher with carbon ions (up to 64%)

RICE: Radiation-Induced Contrast Enhancement, RAIC: Radiation-Associated Image Change.

Table 2. Dose–volume metrics and clinical risk factors.

Factor (type)	Association with injury	Supporting evidence
High radiation exposure to brain tissue (peak dose, mean dose, or large irradiated volumes) (Dosimetric)	Very high focal doses ("hotspots"), higher average brain dose, or large brain volumes exposed to ≥60–70 Gy are associated with a substantially increased risk of temporal-lobe injury and radiation necrosis.	Dose–volume analyses consistently identify excessive focal or volumetric brain exposure as a principal predictor of temporal-lobe toxicity.
Excessive dose to small brain subvolumes (>57.6 Gy RBE to ≥1% of the CNS) (Dosimetric)	Even limited high-dose exposure to a small proportion of brain tissue markedly increases the risk of RICE/RAIC, with symptomatic injury more likely beyond this threshold.	Prospective proton-therapy cohorts demonstrate that >57.6 Gy RBE to ≥1% of the CNS is an independent predictor of RICE.
Very high-dose exposure to very small volumes (≥70 Gy RBE to ≥0.17 cc) (Dosimetric)	When ≥0.17 cc of brain tissue receives ≥70 Gy RBE, the probability of developing RAIC rises sharply, approaching ~63%.	Head-and-neck proton-therapy series report RAIC incidences of approximately 63% when this dose–volume constraint is exceeded.
Older age (Patient)	Age-related microvascular fragility and diminished repair capacity increase susceptibility to delayed radiation necrosis.	Clinical series consistently report higher rates of necrosis and symptomatic injury in older patients.
Pre-existing comorbidities (diabetes, hypertension) (Patient)	Chronic vascular disease exacerbates endothelial injury and increases vulnerability to radiation-induced brain injury.	Patients with metabolic or hypertensive disorders experience higher rates of RICE and necrosis across multiple cohorts.
Prior cranial irradiation (Patient)	Previous radiation exposure markedly increases the risk of necrosis and symptomatic RICE/RAIC during re-irradiation.	Proton-therapy studies show significantly higher injury rates in previously irradiated brain regions.

 doi:10.20944/preprints202601.0677.v1

Concurrent chemotherapy (e.g., temozolomide) (Treatment)	Systemic therapy potentiates inflammatory and vascular responses, increasing the likelihood of pseudoprogression.	Combined chemoradiotherapy regimens consistently demonstrate higher pseudoprogression rates.
Tumour location (Anatomical)	Injury patterns depend on anatomical proximity: clival tumours commonly affect temporal lobes, whereas jugular-foramen lesions may involve the cerebellum or brainstem.	Spatial relationship between tumour targets and adjacent neural structures determines the distribution of radiation injury.

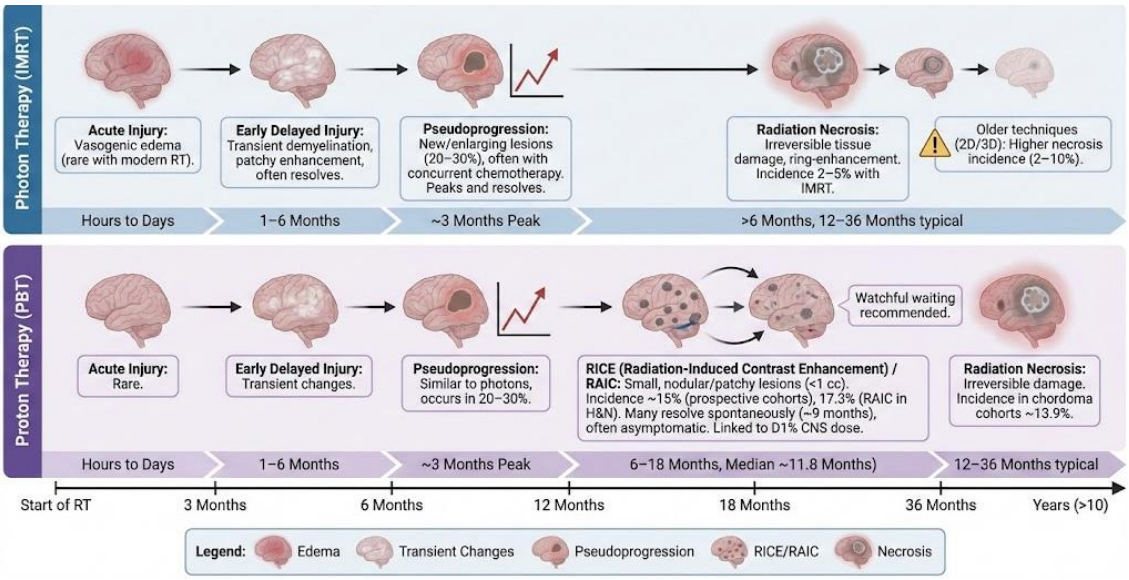

Figure 1. Temporal evolution and radiographic characteristics of radiation-induced brain injury (RIBI) following photon versus proton therapy.

4. Discussion

This review synthesises current knowledge on MRI and PET alterations after proton and photon radiotherapy for adult skull-base tumours. Radiation-induced brain injury results from endothelial damage and inflammatory cascades leading to blood–brain barrier breakdown and necrosis [46]. MRI alterations manifest as pseudoprogression, RICE/RAIC and radiation necrosis, forming a continuum of injury. Pseudoprogression occurs early and often resolves spontaneously [43]. RICE/RAIC lesions appear months later and may regress; many remain asymptomatic [25]. Radiation necrosis is a severe late effect, presenting with ring enhancement and requiring intervention in symptomatic cases [36].

Proton therapy reduces high-dose exposure to temporal and frontal lobes compared with photons, resulting in lower incidence of necrosis. However, RICE/RAIC remains common (15–17%) and typically resolves without treatment [19]. Carbon-ion therapy offers greater biological effectiveness but has higher necrosis rates (up to 64%)[33]. In chordoma and chondrosarcoma, temporal-lobe reactions occur in ~22% and necrosis in ~14%, with risk strongly correlated with Dmax, V70 and patient age. Photon therapy for nasopharyngeal carcinoma and adenoid cystic carcinoma is associated with greater temporal-lobe necrosis due to larger high-dose volumes, though IMRT has lowered rates [47,48]. Risk factors across modalities include high doses to small brain volumes, prior irradiation, older age, diabetes and hypertension [49].

 doi:10.20944/preprints202601.0677.v1

4.1. Clinical Implications

Understanding MRI alterations is critical for patient management. Early identification of pseudoprogression and RICE avoids unnecessary biopsy or premature treatment changes. Misinterpreting RICE as tumor progression can lead to several erroneous medical decisions, including unnecessary surgery, premature discontinuation of effective therapy, and initiation of inappropriate treatments that may worsen outcomes. The most common error is mistaking RICE for tumor recurrence or progression. Studies show that at initial RICE occurrence, 39% of cases were misinterpreted as tumor progression. When RICE is incorrectly diagnosed as progressive disease, patients may undergo unnecessary surgical interventions or biopsy procedures to confirm what is actually a benign treatment effect. This exposes patients to surgical risks without therapeutic benefit [50]. Many RICE lesions resolve spontaneously; thus, short-interval MRI follow-up (3–6 months) is recommended. Advanced MRI and PET improve differentiation between necrosis and recurrence. In uncertain cases, combining multiple modalities (e.g., DWI, PWI, MRS, FET-PET) increases diagnostic confidence.

Dose constraints should be applied rigorously. Based on current evidence, limiting Dmax to the temporal lobe ≤63–66 GyRBE and V70 < 0.17 cc decreases RAIC risk [29]. For chordomas/chondrosarcomas, careful optimization of beam angles and robust planning are required to spare the medial temporal lobe. Diabetes, hypertension and previous irradiation should be considered when balancing tumor control and toxicity. When re-irradiation is needed, proton therapy is preferred to minimize additional brain dose.

4.2. Limitations of Current Evidence

Most data derive from retrospective series with small sample sizes, heterogeneous tumor types and variable follow-up. Definitions of RICE, RAIC, CEBL and necrosis differ across studies, limiting comparability. Many series include both adult and pediatric patients or combine skull-base and non-skull-base tumors. Dosimetric parameters often vary because of differences in planning systems and RBE assumptions. Information on non-proton modalities (e.g., carbon ions) is scarce. Furthermore, many advanced MRI and PET studies focus on gliomas; direct application to skull-base tumors requires caution due to anatomical constraints and differences in tumor biology.

4.3. Future Research

Prospective multicenter studies with standardized imaging protocols and definitions are needed. Integration of radiomics and machine learning may identify early imaging signatures predictive of necrosis. Investigation of biomarkers (e.g., circulating endothelial cells, VEGF levels) could complement imaging. Studies should evaluate the impact of new systemic therapies (e.g., immunotherapy, targeted agents) on pseudoprogression rates. For carbon-ion therapy, exploring dose fractionation and biological optimization may reduce necrosis risk. PET/MRI scanners could enable comprehensive assessment of metabolism and structure in a single session, facilitating adaptive radiotherapy.

5. Conclusions

Radiation-induced brain injury remains a key late effect in skull-base tumor radiotherapy, representing a spectrum from pseudoprogression to necrosis. Advanced MRI and PET imaging aid differentiation from recurrence, while future work should harmonize definitions, integrate radiomics, and optimize dose constraints to reduce toxicity. AI and radiomics may enable us in the future to detect RICE at a very early stage and initiate preventive treatment to minimize the progression to radiation necrosis.

Author Contributions: Conceptualization: G.L., N.P.N.; Methodology: G.L., V.C., D.A.; Formal analysis: G.L., B.N.; Investigation: G.L., V.C., S.M.;Resources: V.C., D.A., B.P.;Data curation: G.L., B.N.;Writing—original draft

 doi:10.20944/preprints202601.0677.v1

preparation: G.L.;Writing—review and editing: G.L., V.C., D.A., N.P.N., B.P.; Visualization: G.L., S.M.;Supervision: N.P.N., B.P.;Project administration: G.L.; All authors have read and agreed to the published version of the manuscript.

Funding: This research received no external funding.

Institutional: Review Board Statement The study did not require ethical approval.

Informed Consent Statement: Not applicable.

Data Availability Statement: Not applicable.

Acknowledgments: AI (GEMINI) was used to generate the Figure 1.

Conflicts of Interest: The authors declare no conflicts of interest.

Abbreviations

The following abbreviations are used in this manuscript: MRI, magnetic resonance imaging; PET, positron emission tomography; RT, radiotherapy; PBT, proton beam therapy; IMRT, intensity-modulated radiotherapy; VMAT, volumetric-modulated arc therapy; RIBI, radiation-induced brain injury; RICE, radiation-induced contrast enhancement; RAIC, radiation-associated image changes; CEBL, contrast-enhancing brain lesions; RBE, relative biological effectiveness; Gy, gray; GyRBE, gray (relative biological effectiveness); CNS, central nervous system; OAR, organ at risk; DWI, diffusion-weighted imaging; PWI, perfusion-weighted imaging; MRS, magnetic resonance spectroscopy; FDG, fluorodeoxyglucose; FET, fluoroethyl-L-tyrosine.

References

1. Rhoton AL. The anterior and middle cranial base. Neurosurgery 2002;51:S273-302.
2. Kockro RA, Schwandt E, Ringel F, Eisenring CV, Nowinski WL. Operative Anatomy of the Skull Base: 3D Exploration with a Highly Detailed Interactive Atlas. J Neurol Surg B Skull Base 2022;83:e298–305. https://doi.org/10.1055/s-0041-1729975.
3. Forst DA, Jones PS. Skull Base Tumors. Continuum (Minneap Minn) 2023;29:1752–78. https://doi.org/10.1212/CON.0000000000001361.
4. Chugh R, Tawbi H, Lucas DR, Biermann JS, Schuetze SM, Baker LH. Chordoma: the nonsarcoma primary bone tumor. Oncologist 2007;12:1344–50. https://doi.org/10.1634/theoncologist.12-11-1344.
5. Stacchiotti S, Sommer J, Chordoma Global Consensus Group. Building a global consensus approach to chordoma: a position paper from the medical and patient community. Lancet Oncol 2015;16:e71-83. https://doi.org/10.1016/S1470-2045(14)71190-8.
6. Otto K. Volumetric modulated arc therapy: IMRT in a single gantry arc. Med Phys 2008;35:310–7. https://doi.org/10.1118/1.2818738.
7. Durante M, Loeffler JS. Charged particles in radiation oncology. Nat Rev Clin Oncol 2010;7:37–43. https://doi.org/10.1038/nrclinonc.2009.183.
8. Lomax AJ, Bortfeld T, Goitein G, Debus J, Dykstra C, Tercier PA, et al. A treatment planning inter-comparison of proton and intensity modulated photon radiotherapy. Radiother Oncol 1999;51:257–71. https://doi.org/10.1016/s0167-8140(99)00036-5.
9. Degrandi-Hoffman G, Eckholm B, Huang M. Methods for comparing nutrients in beebread made by Africanized and European honey bees and the effects on hemolymph protein titers. J Vis Exp 2015:52448. https://doi.org/10.3791/52448.
10. Rampinelli V, Testa G, Arosio AD, Piazza C. Skull base osteoradionecrosis: from pathogenesis to treatment. Curr Opin Otolaryngol Head Neck Surg 2025;33:65–73. https://doi.org/10.1097/MOO.0000000000001036.
11. Lauwens L, Ribeiro MF, Zegers CML, Høyer M, Alapetite C, Blomstrand M, et al. Systematic review of MRI alterations in the brain following proton and photon radiation therapy: Towards a uniform European Particle Therapy Network (EPTN) definition. Radiother Oncol 2025;208:110936. https://doi.org/10.1016/j.radonc.2025.110936.

 doi:10.20944/preprints202601.0677.v1

12. Katsura M, Sato J, Akahane M, Furuta T, Mori H, Abe O. Recognizing Radiation-induced Changes in the Central Nervous System: Where to Look and What to Look For. Radiographics 2021;41:224–48. https://doi.org/10.1148/rg.2021200064.
13. Kim J, Park Y-K, Sharp G, Busse P, Winey B. Water equivalent path length calculations using scatter-corrected head and neck CBCT images to evaluate patients for adaptive proton therapy. Phys Med Biol 2017;62:59–72. https://doi.org/10.1088/1361-6560/62/1/59.
14. Leeman JE, Romesser PB, Zhou Y, McBride S, Riaz N, Sherman E, et al. Proton therapy for head and neck cancer: expanding the therapeutic window. Lancet Oncol 2017;18:e254–65. https://doi.org/10.1016/S1470-2045(17)30179-1.
15. van de Water S, Albertini F, Weber DC, Heijmen BJM, Hoogeman MS, Lomax AJ. Anatomical robust optimization to account for nasal cavity filling variation during intensity-modulated proton therapy: a comparison with conventional and adaptive planning strategies. Phys Med Biol 2018;63:025020. https://doi.org/10.1088/1361-6560/aa9c1c.
16. Balentova S, Adamkov M. Molecular, Cellular and Functional Effects of Radiation-Induced Brain Injury: A Review. Int J Mol Sci 2015;16:27796–815. https://doi.org/10.3390/ijms161126068.
17. Barisano G, Bergamaschi S, Acharya J, Rajamohan A, Gibbs W, Kim P, et al. Complications of Radiotherapy and Radiosurgery in the Brain and Spine. Neurographics (2011) 2018;8:167–87. https://doi.org/10.3174/ng.1700066.
18. Brandes AA, Franceschi E, Tosoni A, Blatt V, Pession A, Tallini G, et al. MGMT promoter methylation status can predict the incidence and outcome of pseudoprogression after concomitant radiochemotherapy in newly diagnosed glioblastoma patients. J Clin Oncol 2008;26:2192–7. https://doi.org/10.1200/JCO.2007.14.8163.
19. Lütgendorf-Caucig C, Pelak M, Hug E, Flechl B, Surböck B, Marosi C, et al. Prospective Analysis of Radiation-Induced Contrast Enhancement and Health-Related Quality of Life After Proton Therapy for Central Nervous System and Skull Base Tumors. Int J Radiat Oncol Biol Phys 2024;118:1206–16. https://doi.org/10.1016/j.ijrobp.2024.01.007.
20. Kumar AJ, Leeds NE, Fuller GN, Van Tassel P, Maor MH, Sawaya RE, et al. Malignant gliomas: MR imaging spectrum of radiation therapy- and chemotherapy-induced necrosis of the brain after treatment. Radiology 2000;217:377–84. https://doi.org/10.1148/radiology.217.2.r00nv36377.
21. Rubin P, Constine LS, Fajardo LF, Phillips TL, Wasserman TH. RTOG Late Effects Working Group. Overview. Late Effects of Normal Tissues (LENT) scoring system. Int J Radiat Oncol Biol Phys 1995;31:1041–2. https://doi.org/10.1016/0360-3016(95)00057-6.
22. Brandes AA, Franceschi E, Tosoni A, Blatt V, Pession A, Tallini G, et al. MGMT promoter methylation status can predict the incidence and outcome of pseudoprogression after concomitant radiochemotherapy in newly diagnosed glioblastoma patients. J Clin Oncol 2008;26:2192–7. https://doi.org/10.1200/JCO.2007.14.8163.
23. Eichkorn T, Lischalk JW, Schwarz R, Bauer L, Deng M, Regnery S, et al. Radiation-Induced Cerebral Contrast Enhancements Strongly Share Ischemic Stroke Risk Factors. Int J Radiat Oncol Biol Phys 2024;118:1192–205. https://doi.org/10.1016/j.ijrobp.2023.12.044.
24. Engeseth GM, Stieb S, Mohamed ASR, He R, Stokkevåg CH, Brydøy M, et al. Outcomes and patterns of radiation associated brain image changes after proton therapy for head and neck skull base cancers. Radiother Oncol 2020;151:119–25. https://doi.org/10.1016/j.radonc.2020.07.008.
25. Engeseth GM, Stieb S, Mohamed ASR, He R, Stokkevåg CH, Brydøy M, et al. Outcomes and patterns of radiation associated brain image changes after proton therapy for head and neck skull base cancers. Radiother Oncol 2020;151:119–25. https://doi.org/10.1016/j.radonc.2020.07.008.
26. Santoni R, Liebsch N, Finkelstein DM, Hug E, Hanssens P, Goitein M, et al. Temporal lobe (TL) damage following surgery and high-dose photon and proton irradiation in 96 patients affected by chordomas and chondrosarcomas of the base of the skull. Int J Radiat Oncol Biol Phys 1998;41:59–68. https://doi.org/10.1016/s0360-3016(98)00031-5.

 doi:10.20944/preprints202601.0677.v1

27. Cheung M, Chan AS, Law SC, Chan JH, Tse VK. Cognitive function of patients with nasopharyngeal carcinoma with and without temporal lobe radionecrosis. Arch Neurol 2000;57:1347–52. https://doi.org/10.1001/archneur.57.9.1347.
28. Viselner G, Farina L, Lucev F, Turpini E, Lungarotti L, Bacila A, et al. Brain MR findings in patients treated with particle therapy for skull base tumors. Insights Imaging 2019;10:94. https://doi.org/10.1186/s13244-019-0784-9.
29. Mattke M, Ohlinger M, Bougatf N, Harrabi S, Wolf RJ, Seidensaal K, et al. Proton and carbon ion beam treatment with active raster scanning method in 147 patients with skull base chordoma at the Heidelberg Ion Beam Therapy Center—a single-center experience. Strahlentherapie Und Onkologie 2022;199:160–8.
30. Pehlivan B, Ares C, Lomax AJ, Stadelmann O, Goitein G, Timmermann B, et al. Temporal lobe toxicity analysis after proton radiation therapy for skull base tumors. Int J Radiat Oncol Biol Phys 2012;83:1432–40. https://doi.org/10.1016/j.ijrobp.2011.10.042.
31. El Shafie RA, Czech M, Kessel KA, Habermehl D, Weber D, Rieken S, et al. Evaluation of particle radiotherapy for the re-irradiation of recurrent intracranial meningioma. Radiat Oncol 2018;13:86. https://doi.org/10.1186/s13014-018-1026-x.
32. Engel D, Schnitzer A, Brade J, Blank E, Wenz F, Suetterlin M, et al. Are mammographic changes in the tumor bed more pronounced after intraoperative radiotherapy for breast cancer? Subgroup analysis from a randomized trial (TARGIT-A). Breast J 2013;19:92–5. https://doi.org/10.1111/tbj.12049.
33. Miyawaki D, Murakami M, Demizu Y, Sasaki R, Niwa Y, Terashima K, et al. Brain injury after proton therapy or carbon ion therapy for head-and-neck cancer and skull base tumors. Int J Radiat Oncol Biol Phys 2009;75:378–84. https://doi.org/10.1016/j.ijrobp.2008.12.092.
34. Ruben JD, Dally M, Bailey M, Smith R, McLean CA, Fedele P. Cerebral radiation necrosis: incidence, outcomes, and risk factors with emphasis on radiation parameters and chemotherapy. Int J Radiat Oncol Biol Phys 2006;65:499–508. https://doi.org/10.1016/j.ijrobp.2005.12.002.
35. Witzmann K, Raschke F, Wesemann T, Löck S, Funer F, Linn J, et al. Diffusion decrease in normal-appearing white matter structures following photon or proton irradiation indicates differences in regional radiosensitivity. Radiother Oncol 2024;199:110459. https://doi.org/10.1016/j.radonc.2024.110459.
36. Zheng Z, Wang B, Zhao Q, Zhang Y, Wei J, Meng L, et al. Research progress on mechanism and imaging of temporal lobe injury induced by radiotherapy for head and neck cancer. Eur Radiol 2022;32:319–30. https://doi.org/10.1007/s00330-021-08164-6.
37. Tringale KR, Nguyen TT, Karunamuni R, Seibert T, Huynh-Le M-P, Connor M, et al. Quantitative Imaging Biomarkers of Damage to Critical Memory Regions Are Associated With Post-Radiation Therapy Memory Performance in Brain Tumor Patients. Int J Radiat Oncol Biol Phys 2019;105:773–83. https://doi.org/10.1016/j.ijrobp.2019.08.003.
38. Barajas RF, Chang JS, Sneed PK, Segal MR, McDermott MW, Cha S. Distinguishing recurrent intra-axial metastatic tumor from radiation necrosis following gamma knife radiosurgery using dynamic susceptibility-weighted contrast-enhanced perfusion MR imaging. AJNR Am J Neuroradiol 2009;30:367–72. https://doi.org/10.3174/ajnr.A1362.
39. Weybright P, Sundgren PC, Maly P, Hassan DG, Nan B, Rohrer S, et al. Differentiation between brain tumor recurrence and radiation injury using MR spectroscopy. AJR Am J Roentgenol 2005;185:1471–6. https://doi.org/10.2214/AJR.04.0933.
40. Rock JP, Hearshen D, Scarpace L, Croteau D, Gutierrez J, Fisher JL, et al. Correlations between magnetic resonance spectroscopy and image-guided histopathology, with special attention to radiation necrosis. Neurosurgery 2002;51:912–9; discussion 919-920. https://doi.org/10.1097/00006123-200210000-00010.
41. Pyka T, Hiob D, Preibisch C, Gempt J, Wiestler B, Schlegel J, et al. Diagnosis of glioma recurrence using multiparametric dynamic 18F-fluoroethyl-tyrosine PET-MRI. Eur J Radiol 2018;103:32–7. https://doi.org/10.1016/j.ejrad.2018.04.003.
42. Zips D, Zöphel K, Abolmaali N, Perrin R, Abramyuk A, Haase R, et al. Exploratory prospective trial of hypoxia-specific PET imaging during radiochemotherapy in patients with locally advanced head-and-neck cancer. Radiother Oncol 2012;105:21–8. https://doi.org/10.1016/j.radonc.2012.08.019.

 doi:10.20944/preprints202601.0677.v1

43. Brandsma D, Stalpers L, Taal W, Sminia P, van den Bent MJ. Clinical features, mechanisms, and management of pseudoprogression in malignant gliomas. Lancet Oncol 2008;9:453–61. https://doi.org/10.1016/S1470-2045(08)70125-6.
44. Kirste S, Treier M, Wehrle SJ, Becker G, Abdel-Tawab M, Gerbeth K, et al. Boswellia serrata acts on cerebral edema in patients irradiated for brain tumors: a prospective, randomized, placebo-controlled, double-blind pilot trial. Cancer 2011;117:3788–95. https://doi.org/10.1002/cncr.25945.
45. Cai X, Li P, Zhao J, Wang W, Cheng J, Zhang G, et al. Definitive carbon ion re-irradiation with pencil beam scanning in the treatment of unresectable locally recurrent rectal cancer. J Radiat Res 2023;64:933–9. https://doi.org/10.1093/jrr/rrad068.
46. Tsao MN, Li YQ, Lu G, Xu Y, Wong CS. Upregulation of vascular endothelial growth factor is associated with radiation-induced blood-spinal cord barrier breakdown. J Neuropathol Exp Neurol 1999;58:1051–60. https://doi.org/10.1097/00005072-199910000-00003.
47. Peng G, Wang T, Yang K-Y, Zhang S, Zhang T, Li Q, et al. A prospective, randomized study comparing outcomes and toxicities of intensity-modulated radiotherapy vs. conventional two-dimensional radiotherapy for the treatment of nasopharyngeal carcinoma. Radiother Oncol 2012;104:286–93. https://doi.org/10.1016/j.radonc.2012.08.013.
48. Zhou G-Q, Yu X-L, Chen M, Guo R, Lei Y, Sun Y, et al. Radiation-induced temporal lobe injury for nasopharyngeal carcinoma: a comparison of intensity-modulated radiotherapy and conventional two-dimensional radiotherapy. PLoS One 2013;8:e67488. https://doi.org/10.1371/journal.pone.0067488.
49. Quigg M, Yen C-P, Chatman M, Quigg AH, McNeill IT, Przybylowski CJ, et al. Risks of history of diabetes mellitus, hypertension, and other factors related to radiation-induced changes following Gamma Knife surgery for cerebral arteriovenous malformations. J Neurosurg 2012;117 Suppl:144–9. https://doi.org/10.3171/2012.6.GKS1245.
50. Eichkorn T, Lischalk JW, Sandrini E, Meixner E, Regnery S, Held T, et al. Iatrogenic influence on prognosis of radiation-induced contrast enhancements in patients with glioma WHO 1-3 following photon and proton radiotherapy. Radiother Oncol 2022;175:133–43. https://doi.org/10.1016/j.radonc.2022.08.025.